

Analysis of QUENCH-ACM Experiments using SCDAP/RELAP5

J. Birchley

Paul Scherrer Institute, Switzerland

TEL: +41 56 310 2724, FAX: +41 56 310 2199; Email: jonathan.birchley@psi.ch

J. Stuckert

Karlsruhe Institute of Technology, Germany

TEL: +49 7247 82 2558, Fax: +49 7247 82 2095; Email: juri.stuckert@kit.edu

Abstract - The QUENCH experimental programme at Karlsruhe Institute of Technology (formerly Forschungszentrum Karlsruhe (FZK)) investigates heat-up and reflooding of a core under severe accident conditions, but while the geometry is still mainly rod-like. The recent QUENCH-ACM series of experiments, comprising QUENCH-12 (E110), -14 (M5[®]) and -15 (Zirlo[™]), together with QUENCH-06 (reference case, Zry4) addressed the effect of alternative cladding materials on oxidation and quenching under similar conditions. The cladding material and bundle configuration reflected different reactor core designs, namely VVER, EPR, Westinghouse AP-1000 and Siemens Konvoi, respectively. Superficial inspection of the experimental results reveals only minor differences in the thermal and oxidation response, except for the much larger hydrogen release during reflood in QUENCH-12. Post-test calculations were performed using a version of SCDAP/RELAP5/MOD3.2, modified to represent the QUENCH facility and to invoke alternative oxidation correlations. The calculations agreed rather well with experiments QUENCH-06, -14 and -15 but the significant hydrogen release during reflood in QUENCH-12 was not captured. Closer examination of the experimental results reveals further differences between QUENCH-12 which may be linked to breakaway oxidation of the E110 cladding, for which there is evidence from post-test inspection. Sensitivity studies using the Sokolov correlation (for E110) and a trial correlation for M5 indicate no improvement over the SCDAP standard correlation (Cathcart-Pawel/Urbanic-Heidrick). The analyses support the heuristic observation that there was no major difference between the influence of Zircaloy-4, M5 or Zirlo, but the E-110 exhibited a contrasting behaviour with a consequent impact on the reflooding.

I. INTRODUCTION

The trend toward operating to higher burnup and the need to minimise corrosion of the fuel cladding have motivated the use of so-called "advanced" niobium-bearing cladding alloys (E-110, M5[®], Zirlo[™]), which are claimed to possess improved resistance to corrosion compared with the tin-bearing Zircaloy-4 currently used in the large majority PWRs. While there is a wealth of data and several alternative correlations for Zircaloy-4 oxidation characteristics [1,2,3,4,5], data for the advanced cladding alloys are comparatively scarce. To remedy this shortfall, the NUKLEAR programme at Karlsruhe Institute of Technology (KIT) has been conducting a systematic investigation of oxidation behaviour of the different cladding alloys, via separate effects experiments [6]. In

parallel, the QUENCH-ACM series [7] was launched to address the effect of cladding alloy on the heat-up, oxidation and quenching under similar thermal and hydraulic transient conditions. Thus the experiments QUENCH-12 [8], -14 [9] and -15 [10], together with the reference case QUENCH-06 [11] provide data on E-110, M5[®], Zirlo[™] and Zircaloy-4 used or planned for use in VVER, EPR, AP1000 and Konvoi plants, respectively. Trial correlations for oxidation kinetics have been derived from separate effects experiments on the different materials [12].

This paper is a companion to a paper at the present conference describing the experimental results of QUENCH-15 [13]. The present investigation comprises an interim post-test analysis of the QUENCH-ACM experiments, using SCDAP/RELAP5/MOD3.2 which is

used by Paul Scherrer Institute (PSI) as one of the tools to analyse Beyond-Design Basis Accidents in nuclear plants. A brief summary of the test train and experiment, concentrating on test-to-test comparison of key features and results, are in section II. The computational models and post-test analyses are described in section III. Tentative conclusions are presented in section IV.

II. SUMMARY OF QUENCH-ACM EXPERIMENTS

The QUENCH facility is constructed to investigate the hydrogen source term resulting from water injection into an uncovered core of a Light Water Reactor as well as the high-temperature behaviour of core materials under transient conditions. The test bundle is of total length of approximately 2.5 m and is shown schematically in Fig. 1a. The QUENCH-06 and -14 bundles consisted of 20 fuel rod simulators and one centrally located unheated rod, arranged in a rectangular area as shown in Fig. 1b. The configuration differed in QUENCH-12 (Fig. 1c) in that

there were 18 heated and 13 unheated rods arranged in a hexagonal array, while there were 24 heated rods arranged in a rectangular array in QUENCH-15 (Fig. 1d). The rod diameter, pitch and arrangement reflected the respective plant core configuration. It is noted that although different Zr-based materials were used for the cladding, the QUENCH-14, shroud was made from the same Zry-4 as in QUENCH-06, while the QUENCH-12 shroud was made from a Zr-2.5%Nb alloy which has similar properties to E-110 (Zr-1%Nb). The QUENCH-15 shroud was made from Zr-702 (Zr with 4.5wt% Hf). Since the shroud inner surface is about 30% of the total, any differences between the oxidation kinetics of Zry-4 and the different materials would have been masked slightly in QUENCH-14 and QUENCH-15. The shroud inner radius and thickness of insulation were slightly different in QUENCH-12 and -15 compared with the other experiments, to accommodate the larger number of rods.

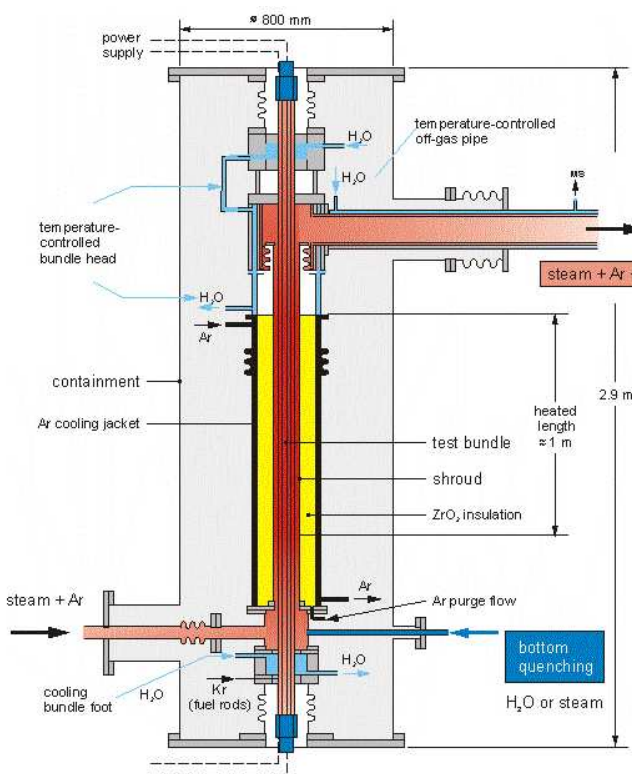


Fig. 1a: Schematic of the QUENCH facility

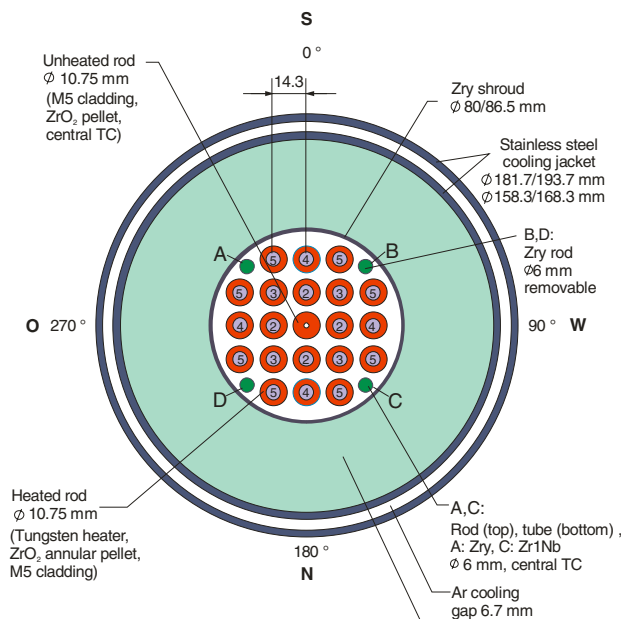


Fig. 1b: Cross section of the QUENCH-06 and -14 bundles

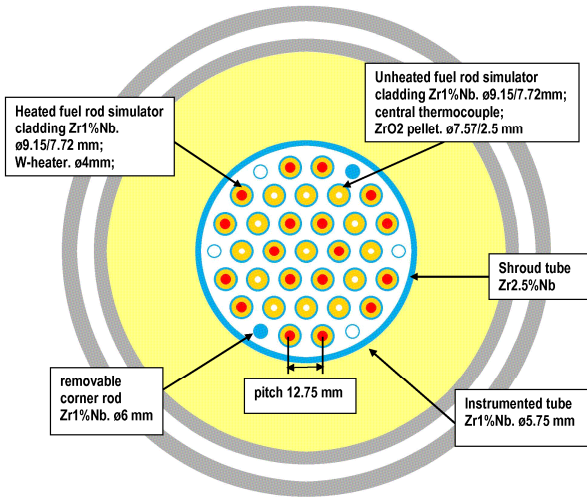


Fig. 1c: Cross section of the QUENCH-12 bundle

A test objective of each of the QUENCH-ACM experiments was to achieve pre-reflood thermal and hydraulic transient conditions as close as practical to QUENCH-06, in order to examine the oxidation characteristics of the different claddings under similar conditions. A general account of the QUENCH facility and programme are given in [14]. The experiment conduct comprised five phases: stabilisation of the facility to

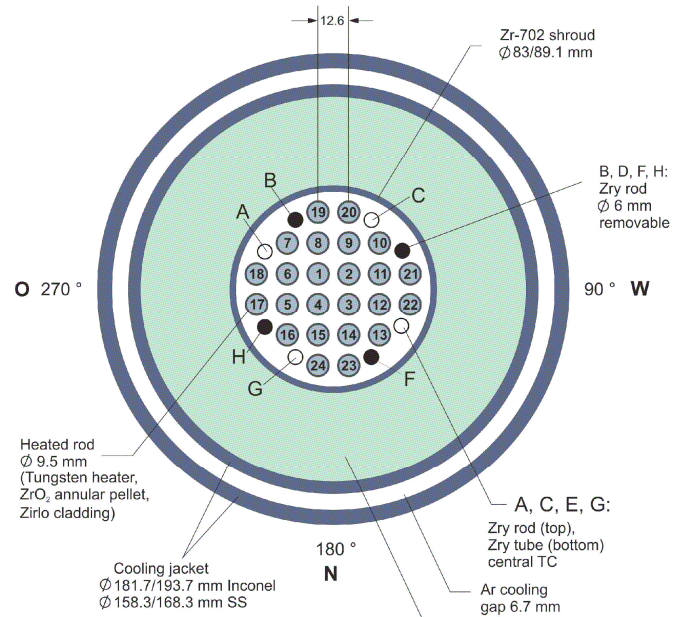


Fig. 1d: Cross section of the QUENCH-15 bundle

establish initial conditions, a first power ramp to reach ca. 1200 °C, a nearly constant temperature plateau to achieve a desired degree of oxidation, a thermal transient during which the power was ramped to achieve a maximum temperature of ca. 1800 °C, and reflood by bottom injection and reduced electrical power. QUENCH-14 typifies the test conduct, which is illustrated schematically in figure 2.

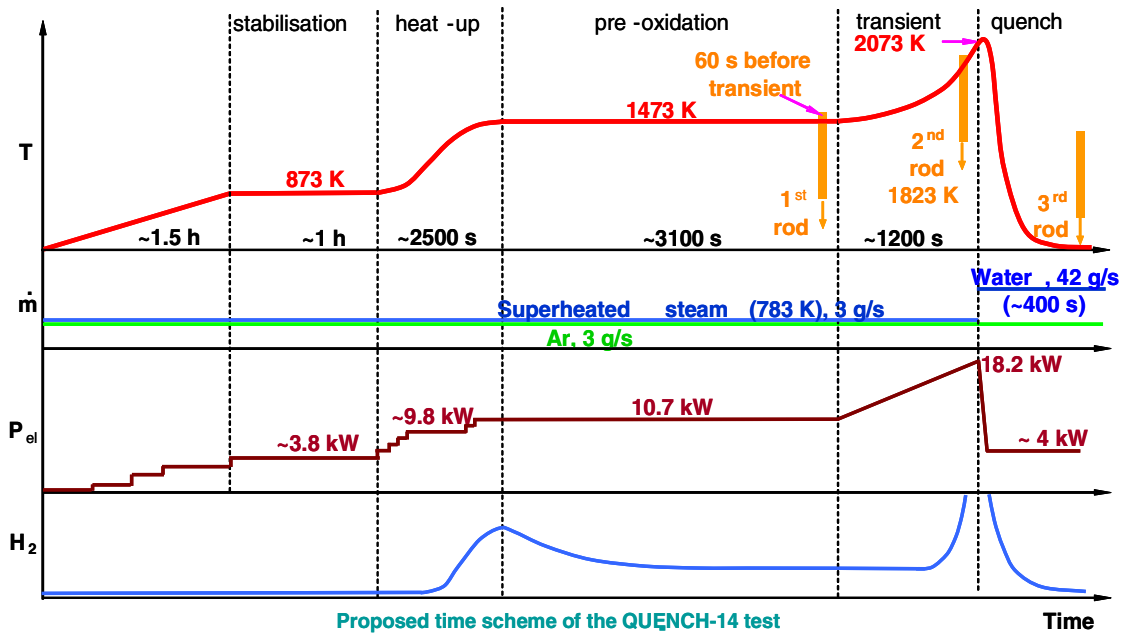


Fig. 2: Outline of QUENCH-14 test conduct

The main characteristics of the experiments are compared by the parameters below in Table I.

TABLE I: Comparison of QUENCH-ACM test parameters

Test	Q-06	Q-12	Q-14	Q-15
Number of rods (heated + unheated)	20 + 1	18 + 13	20 + 1	24 + 0
Flow area (cm ²)	30.1	32.8	30.1	34.6
Normalised wetted surface area	1	1.22	1	1.09
Flow rate (kg/s)				
steam	3.0	3.3	3.0	3.5
argon	3.0	3.3	3.0	3.45
water	42	48	42	48
End of plateau power (kW)	10.9	9.9	11.2	11.6
temperature (K)	1423	1390	1425	1434
Injection time (s)	7179	7270	7213	7120
temperature. (K)	2151	2206	2202	2153
H2 (normalised) (g)				
end of plateau	18	13 (10)	16	23 (21)
transient	14	21 (17)	17	17 (16)
reflood	4	24 (20)	7	8 (7)
total	36	58 (47)	40	48 (44)

The bundle flow rates were slightly higher in QUENCH-12 and -15 to account for the larger bundle flow area, while the injection rates also higher. The power was controlled at different levels in order to achieve similar temperatures during the plateau phase in the four tests. This was necessary to compensate differences in the thermal capacity, flow area and heat transfer area of the bundle, and the geometry of the electrical heating. Thus the temperature at the hottest elevation on the shroud during this phase was approximately constant at ca. 1400 K. The test to test variations of up to 50 K were about the same as the azimuthal variations in shroud temperature, which arose mainly from unintended inhomogeneities in the flow conditions and are an indication of the experimental uncertainty. The deployment of bundle thermocouples is not identical in every test which makes test to test comparison more difficult. It is noted also that slightly higher temperatures were sometimes observed on some of the heater rods, but the shroud and corner rod temperatures, measured by thermocouples without contact with steam, were more reliable. In each case the pre-oxidation plateau continued

until 6000 s, when the transient was initiated by ramping the power until the temperature criterion for water injection was reached. Although this was nominally the same in each test, the very exacting conditions meant that the time and temperature at which injection was initiated differed from test to test.

Despite the similarity in thermal hydraulic conditions, there were noticeable differences in the observed hydrogen generation during all three phases, and which are attributable to four main factors: (i) bundle configuration, most notably the oxidisable surface area; (ii) boundary conditions, (iii) experimental uncertainty; (iv) properties of the cladding alloys. Since the oxidation kinetics are rather sensitive to temperature (an increase from 1400 to 1450 K implies about 30% increase in oxidation rate), the remaining variation may be due to any or all of other three factors. The following section describes the comparative analyses performed to examine these effects, in particular to identify a possible influence of cladding material.

III. MODELLING OF QUENCH-ACM EXPERIMENTS

A modified version [15] of SCDAP/RELAP/MOD3.2 (S/R5) [16] has been used extensively in planning and analyses of the QUENCH experiments [17]. The code version contains modifications by FZK for the QUENCH heater element (W) and electrode (Mo, Cu) materials, the ZrO₂ fuel pellet simulator and the shroud insulation. As well as the Cathcart-Pawel/Urbanic-Heidrick (CP/UH) correlations for Zircaloy-4 in the standard code, sub-versions enabled alternative correlations, namely Sokolov for E-110 [18] and a trial correlation for M5[®] [12], coupled with UH. The correlations for the rate of mass gain per unit area are:

Cathcart-Pawel

$$d(m^2)/dt = 33.6 * \exp(-20065/T), \quad T < 1853;$$

Urbanic-Heidrick

$$d(m^2)/dt = 10.85 * \exp(-16610/T), \quad T > 1853;$$

Sokolov

$$d(m^2)/dt = 318.0 * \exp(-23040/T), \quad T < 1773;$$

$$d(m^2)/dt = 196.5 * \exp(-20800/T), \quad T > 1773;$$

M5

$$d(m^2)/dt = 0.64 * \exp(-17541/T), \quad T < 1298;$$

$$d(m^2)/dt = 38.8 * \exp(-20340/T), \quad 1298 < T < 1853.$$

The units are kg² m⁻⁴ s⁻¹ and Kelvins.

It is clear that all the correlations are parabolic, while the M5 correlation gives slower kinetics at T < 1298 K than CP but is similar at T > 1298 K. The Sokolov kinetics are slower than CP at T < 1773 K and comparable with UH at T > 1773 K. All the correlations as applied

give faster kinetics above the tetragonal-cubic phase transition at ca. 1800 K, but only M5 gives slower kinetics below the monoclinic-tetragonal phase transition at ca. 1300 K. Modelling of oxidation at these lower temperatures is an area of current debate, since the kinetics tend towards cubic rather than parabolic provided the protective oxide layer remains stable. However, the oxide layer is susceptible to breakaway to an extent that appears to depend on the cladding type and possibly also on the current and past oxidation conditions.

The input model comprises a single hydraulic channel for the test train including the lower and the upper volumes and offgas line. The cooling systems for the bundle and offgas are also modelled as well as containment and lab environment as thermal boundaries. Sixteen axial nodes are used for the test train, of which ten are for the 1020 mm tungsten heated section, while two/one nodes represent the molybdenum/copper electrodes below the tungsten section, and similarly above it. The noding of the hydraulic volumes, junctions and boundary condition, and the SCDAP components is shown in figure 3.

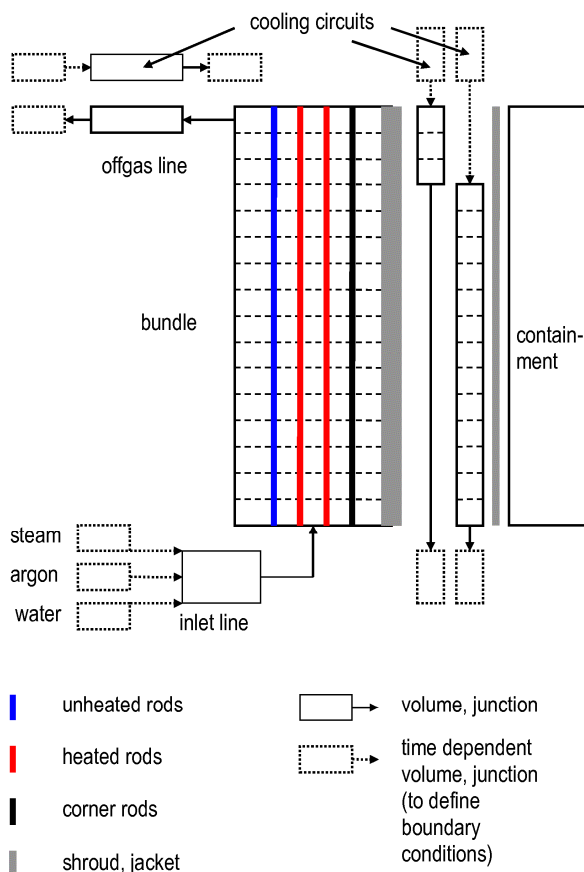


Fig. 3: SCDAP/RELAP5 noding for QUENCH

The bundle components are represented by unheated rods and heater rod simulators as indicated in Table II.

Table II: SCDAP model: bundle components

	Q-06/-14	Q-12	Q-15
Unheated rods	1	1, 12	-
Heated rods	8, 12	6, 12	4, 8, 8, 4
Corner rods	4	6	8

The approach adopted was to model all the tests in as similar a way as possible, with any changes restricted to experimental configuration and conditions. Thus an identical model was used for QUENCH-06 and -14 but modifications were made to take account of the bundle geometry of QUENCH-12 and -15, specifically the number of rod components and rods within each component, the bundle flow area, hydraulic diameter and shroud dimension. The boundary conditions were defined to coincide with the experimental conditions of each test, specifically the electrical power history, the steam, argon, water flow rates. Other conditions (lab temperature, operation of cooling system, inlet gas temperature) were kept the same for each test. The same material properties were used for the hardware in all four tests, typically with values specified in the experimental reports. The CP/UH oxidation correlations were used in base case calculations for all the tests. Part of the reason for this is that the trial correlations resulting from the separate effects tests on the different cladding alloys [12] show similarity to CP at temperatures between 1300 and 1700 K, though with larger differences at lower temperatures. To examine the possible role of cladding on material, additional calculations were performed using the trial M5 correlation, and also with Sokolov for QUENCH-12.

An exception to the above approach was the external electrical resistance, where part of the total electrical power is dissipated and hence does not contribute to the bundle heating. The resistance is typically estimated experimentally at close to 4 mΩ/rod but varies from test to test due to the uncertain contact resistance between the power cables and heater electrodes, and the different external circuitry associated with the three heater rod arrangements. The resistance in the model was adjusted slightly in order to yield a maximum bundle temperature close to the measured value at the start of water injection, so as to avoid a gross under- or over-estimate that would otherwise compromise the analyses of the reflood phase.

IV. RESULTS OF QUENCH-ACM CALCULATIONS AND COMPARISON WITH EXPERIMENT

The total power used in the calculations is defined according to the gross experimental power and is shown in figure 4, together with the calculated power dissipated

in the heater rods (i.e. excluding the external resistance). The convention adopted here and in all the remaining figures is to display experimental data with solid lines and calculated results with dashed lines. Where results are displayed for all four experiments, the colours black/red/green/blue correspond respectively to QUENCH-06/QUENCH-12/QUENCH-14/QUENCH-15.

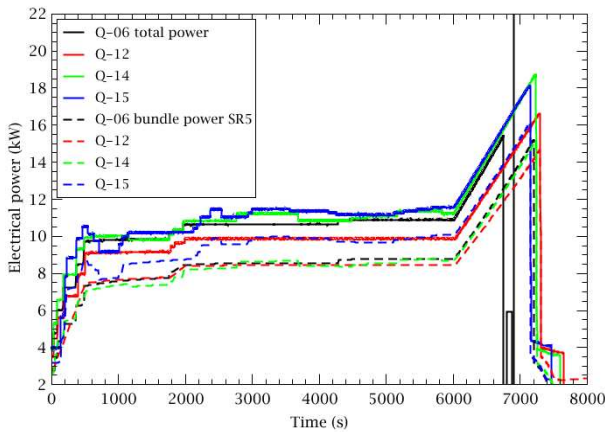


Fig. 4: Gross power and calculated bundle power

The test to test differences indicate the effect of bundle configuration. The timings of power reduction (shortly after reflood initiation) differ by about 150 s due to differences in the time for the bundle heat up from the plateau temperature to the reflood initiation criterion. The main test parameters are shown in Table III which compares the calculated and measured temperature and mass of hydrogen generation at key times in each test. During the pre-oxidation the choice of oxidation model has a significant influence on hydrogen generation, as might be expected, but only a minor effect on the temperature. Figure 5 compares the base case calculated temperatures with the data at the 950 mm elevation. There was a slight overestimate of the plateau temperature QUENCH-15, but generally agreement was good. The test to test variations of ca. 50 K fairly well matched by the calculations, despite the spatial variations in temperature within the bundle that cannot be captured by the model.

The calculations and data for QUENCH-06, -14 and -15 also show the same consistent trend during the plateau, in that the temperatures reached a maximum between 3000 and 3500 s before decrease slightly to a shallow minimum at 6000 s, the start of the power ramp. The reason for this behaviour was the reducing contribution from oxidation heat as the protective oxide layer built up. In attempt to limit this reduction, the power was increased slightly, most notably in QUENCH-06 and -14. A different trend is observed in QUENCH-12 which, instead of decreasing, showed a slight increase in temperature

with the power constant between 3000 and 6000 s. This small but noticeable difference was not calculated.

TABLE III: Measured and calculated parameters

Test	Q-06	Q-12	Q-14	Q-15
T₆₀₀₀				
expt	1423	1390	1425	1434
CP/UH	1441	1391	1430	1474
M5	1432	1384	1422	1464
Sokolov	-	1373	-	-
T_{reflood}				
expt	2151	2206	2202	2153
CP/UH	2126	2215	2249	2143
M5	2261	2659	2421	2250
Sokolov	-	2670	-	-
T_{peak}				
expt	2151	2319	2308	2155
CP/UH	2141	2287	2344	2160
M5	2261	2659	2421	2267
Sokolov	-	2873	-	-
H₂, 6000				
expt	18	13	16	23
CP/UH	18.5	15.7	17.2	24.9
M5	13.7	10.5	12.7	18.1
Sokolov	-	9.4	-	-
H₂,reflood				
expt	32	34	34	41
CP/UH	30.7	27.0	31.5	38.3
M5	28.5	28.5	30.2	34.4
Sokolov	-	24.1	-	-
H₂,final				
expt	36	58	40	48
CP/UH	33.9	31.7	39.7	40.7
M5	33.4	35.8	36.2	36.7
Sokolov	-	34.8	-	-

The base case calculated and measured hydrogen masses are shown in figure 6. Again, overall agreement is good during the experiments, though with a slight overestimation during the pre-oxidation in QUENCH-12, -14 and -15 but a slight underestimation during the subsequent heat-up; these discrepancies are larger in QUENCH-12. A contrasting trend is seen in calculations using M5 correlation, with an underestimation during pre-oxidation; good agreement during the transient was partly due to the overestimated temperature at reflood initiation.

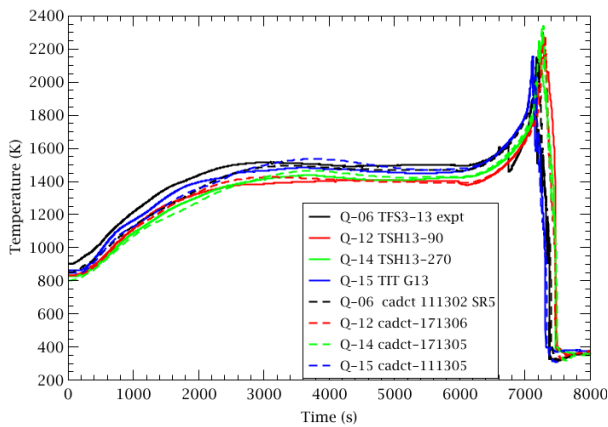


Fig. 5: Measured and calculated temperatures at 950 mm

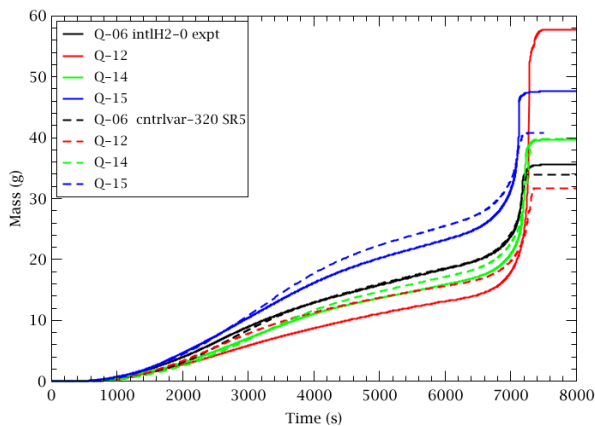


Fig. 6: Measured and calculated hydrogen generation

The measurements of hydrogen are rather uncertain during reflood, but the calculations correctly reproduced the minor release in QUENCH-06, -14 and -15, but failed to capture the much greater release in QUENCH-12. In order to analyse this case more closely, figures 7 and 8 compare the thermal and hydrogen generation histories with the calculations using all three oxidation models. Despite the insensitivity of plateau temperature to the choice of oxidation model, there was a noticeable effect on hydrogen generation, with a 30 to 40% reduction during pre-oxidation when using the M5 and Sokolov correlation. This trend was later reversed since the M5 and Sokolov correlations resulted in much higher temperatures at initiation of reflood. It is at first sight surprising that the alternative correlations gave no clear improvement over CP/UH. In fact agreement was slightly worse with M5, and also with Sokolov for QUENCH-12, although the discrepancy is perhaps not significant when variations and uncertainties are considered. The small hydrogen release during reflood in QUENCH-06, -14, -15 was adequately reproduced by both CP/UH and M5. However, none of the correlations captured the larger

release during reflood in QUENCH-12, despite the high temperatures calculated when M5 and Sokolov were used.

The explanation of the much greater oxidation during reflood in QUENCH-12 may be deduced from examinations of the bundle [8] which showed differences compared with the other tests. The corner rods showed extensive signs of cracks and breakaway oxidation, observed also on the E-110 corner rods in the QUENCH-15 bundle but to a much smaller extent on the Zirlo cladding not at all on Zircaloy-4 or M5. One factor affecting the hydrogen release during QUENCH-12 was the much larger uptake of hydrogen in the remaining metallic, due to its ready access to the metal surface via the network of cracks. However, it was estimated that release during reflood of previously taken-up hydrogen could account for only about 4 g of the 24 g [19]. The maximum temperatures reached were sufficient for metallic melting, but significant release of melt to the sub-channels and melt oxidation was observed only in QUENCH-12, due to failure of the much weaker damaged oxide scale. It is noted that the models in SCDAP/RELAP5 take no account of enhanced oxidation when metallic melt is released to the flowing steam – in fact none of the reactor safety analysis codes models this phenomenon.

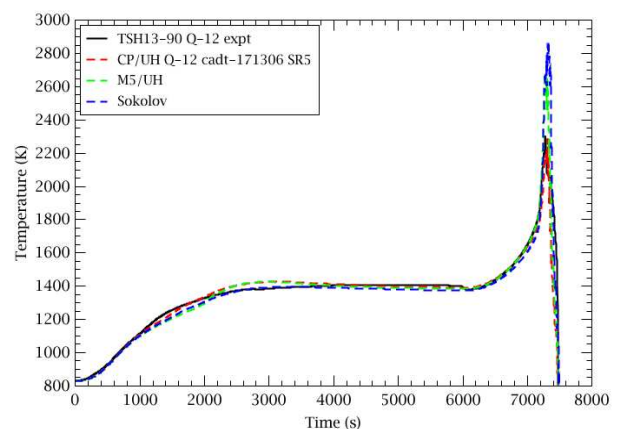


Fig. 7: Effect of oxidation model on temperatures at 950 mm during QUENCH-12

Although release of hydrogen taken up during pre-oxidation was not enough to explain the much larger release during reflood, it may have been a factor during pre-oxidation. Breakaway might possibly have reduced the protective effect of the oxide sufficiently to result in slightly non-parabolic kinetics, suggested by the nearly constant rate of hydrogen release during the pre-oxidation, instead of the decreasing rate calculated by SCDAP and observed in the other tests. However, the effect is small might have been influenced by take-up of hydrogen.

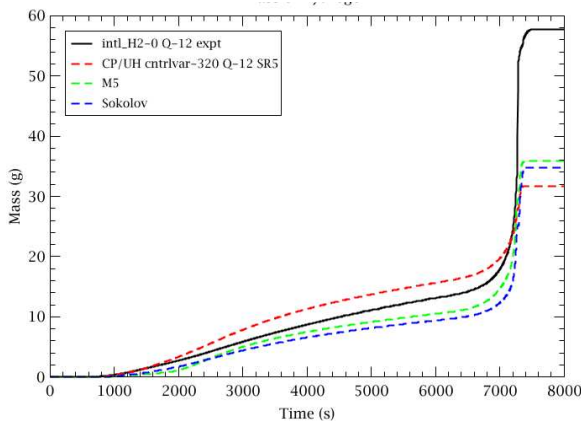


Fig. 8: Effect of oxidation model on hydrogen release during QUENCH-12

Analysis of reflooding is difficult due to a number of factors. The shroud was breached at about the time of reflood initiation in QUENCH-06, -12 and -14, and several thermocouples did not give reliable readings because of the extreme conditions. Also the injection was preceded by rapid refilling of the lower volume. This resulted in an initial surge of water through the bundle, which is not possible to model reliably but caused some cooling and quenching of the rods. These factors tend to compromise any comparison between calculations and data for the quench progression. Apart from a tendency for the calculations to underestimate the early cooling mentioned above, the calculated reflooding and quenching of the shroud are in fairly good agreement with data, as illustrated in figure 9 for QUENCH-14 which typical of the test series.

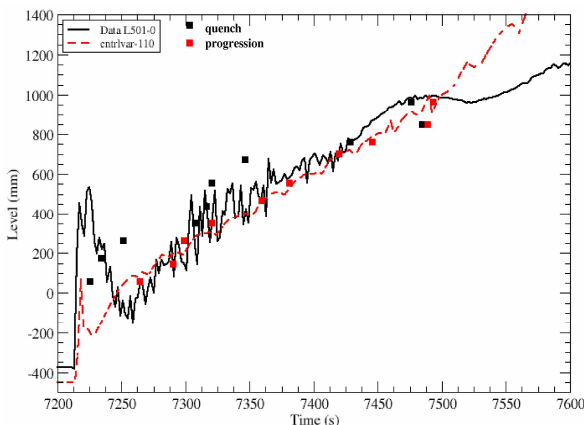


Fig. 9: Measured and calculated progression of reflood and shroud quenching during QUENCH-14

All of the tests showed a cooling trend throughout the bundle which began soon after the start of injection, although there was a longer delay in the upper part of the

bundle during QUENCH-12 compared with the other tests shown in figure 10. The longer delay was not calculated and may be linked to the blockage and/or the continued oxidation. However, the cooling rates and quench times at 950 mm were otherwise in quite good agreement.

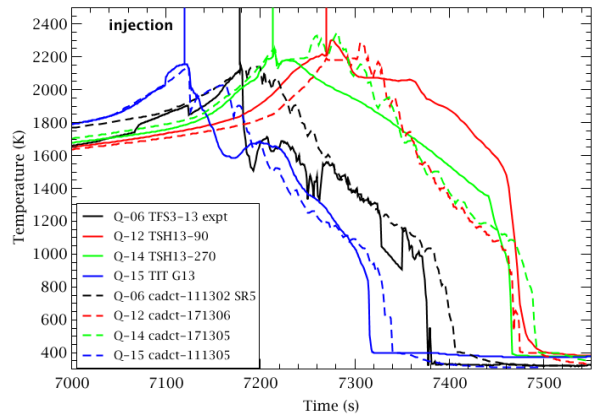


Fig. 10: Measured and calculated temperatures at 950 mm during reflood

V. CONCLUSIONS

Experiments QUENCH-06, -12, -14 and -15 were conducted to address the effect of cladding material on oxidation and reflood. Differences in the bundle configuration and boundary conditions between the tests mean that the effect of cladding material cannot be deduced by direct comparison of the results. A comparative analysis of QUENCH-06, -12, -14 and -15 was therefore performed by means of counterpart calculations using a version of SCDAP/RELAP5/MOD3.2.

The standard CP/UH correlations enabled uniformly good agreement for the thermal histories throughout all four tests. Good agreement was obtained also for the hydrogen generation, except during the reflood phase of QUENCH-12. This discrepancy is linked to the observed oxidation of metallic melt, released through the damaged oxide layer; these phenomena were not modelled.

The behaviour in QUENCH-06, -14 and -15 was very similar, and differences can be attributed to the different configurations and boundary conditions. The analyses suggest there was no major influence of cladding material on the thermal heat-up, oxidation and reflood.

QUENCH-12 also exhibited broadly similar during the pre-reflood phases behaviour, although there was a small but noticeable difference in both the thermal evolution and hydrogen release, not captured in any of the calculations. This is possibly the result of breakaway oxidation and hydrogen take-up in the unoxidised metallic cladding, which are not modelled, and for which

there is evidence from post-test examination. The poorer agreement for QUENCH-12 than the other tests points to a different behaviour of the E-110 cladding.

A trial correlation for M5[®] was used in additional calculations for each test, while Sokolov was used also for QUENCH-12. There was no clear improvement compared with CP/UH but, except for QUENCH-12 reflood, all the calculations are consistent with the data, bearing in mind the experimental incertitude.

The analysis is presently at an interim stage, pending the full experimental reports for QUENCH-14 and -15.

ACKNOWLEDGMENTS

The authors are pleased to thank Swissnuclear and HGF Programme NUKLEAR for significant financial support to conduct these research activities and the QUENCH team at KIT for valuable discussion and technical input.

NOMENCLATURE

ACM	Advanced Cladding Material
CP	Cathcart-Pawel
E110	Russian cladding alloy Zr1%Nb
FZK	Forschungszentrum Karlsruhe
KIT	Karlsruhe Institute of Technology
PSI	Paul Scherrer Institute
PWR	Pressurised Water Reactor
UH	Urbanic-Heidrick
VVER	Vodo-Vodyanoi Energetichesky Reactor (PWR of Russian type)

REFERENCES

1. J. V CATHCART, R.E. Pawel, et al., "Zirconium Metal-Water Oxidation Kinetics, IV: Reaction Rate Studies", ORNL/NUREG-17, (1977).
2. S. LEISTIKOW and G. Schanz, "Oxidation kinetics and related phenomena of Zircaloy-4 fuel cladding exposed to high temperature steam and hydrogen-steam mixtures under PWR accident conditions", *Nucl. Eng. Des.* **103**, 65–84 (1987).
3. V. F. URBANIC and T. R. Heidrick, "High-temperature oxidation of Zircaloy-2 and Zircaloy-4 in steam", *J. Nucl. Mater.* **75**, 251–261(1978).
4. G. SCHANZ, B. Adroguer and A. Volchek, "Advanced treatment of Zircaloy cladding high-temperature oxidation in severe accident code calculations, Part I. Experimental database and basic modeling", *Nucl. Eng. Des.* **232**, 75–84 (2004).
5. A. VOLCHEK, Y. Zvonarev and G. Schanz, "Advanced treatment of Zircaloy cladding high-temperature oxidation in severe accident code calculations, Part II. Best-fitted parabolic correlations", *Nucl. Eng. Des.* **232**, 85-96 (2004).
6. M. STEINBRUECK, "Oxidation of Zirconium Alloys in Oxygen at High Temperatures up to 1600 °C", *Oxidation of Metals* **70**, 317-329 (2008).
7. L. SEPOLD et al., 2007, "Severe Fuel Damage Experiments with Advanced Cladding Materials to be performed in the QUENCH Facility, paper ICONE16-48074, *Proceedings of the 16th International Conference on Nuclear Engineering (ICONE-16)*, Orlando, FL, USA (May 2007)
8. J. STUCKERT et al, "Results of the QUENCH-12 Experiment on Reflood of a VVER-type Bundle", FZKA 7307, Forschungszentrum Karlsruhe Report, (September 2008).
9. J. STUCKERT, et al, "Experimental Results of Reflood Bundle Test QUENCH-14 with M5[®] Cladding Tubes", *Proceedings of the 17th International Conference on Nuclear Engineering (ICONE-17)*, Brussels, Belgium (July, 2009).
10. J. STUCKERT, et al, "Results of Reflood Bundle Test QUENCH-15 with Zirlo[™] Cladding Tubes, 15th Int. QUENCH Workshop, ISBN 978-3-923704-71-2, Karlsruhe, Germany, (November 2009).

11. L. SEPOLD et al, "Experimental and Computational Results of the QUENCH-06 Test (ISP-45)", Forschungszentrum Karlsruhe report FZKA 6664 (2004).
12. M. GROSSE, "Comparison of the High Temperature Steam Oxidation Kinetics of Advanced Cladding Materials", *Proceedings of International Congress on Advances in Nuclear Power Plants (ICAPP '08)*, Anaheim, CA, USA (June 2008).
13. J. STUCKERT, M. Grosse, M. Steinbrueck, "Experimental Results of Reflood Bundle Test QUENCH-15 with ZIRLO™ Cladding Tubes", *Proceedings of International Congress on Advances in Nuclear Power Plants (ICAPP '10)*, San Diego, CA, USA (June, 2010).
14. L. SEPOLD et al, "Severe Fuel Damage Experiments performed in the QUENCH Facility with 21-Rod Bundles of LWR-Type", *Nucl. Eng. Des.* **237**, 2157-2164 (2007).
15. W. HERING and Ch. Homann, "Improvement of the SCDAP/RELAP5 Code with Respect to FZK Experimental Facilities", Forschungszentrum Karlsruhe Report FZKA 6566 (1997).
16. L. SIEFKEN et al., "SCDAP/RELAP5/MOD3.2 Code Manual", NUREG/CR-6150 Rev. 1, INEL-96/0422 Rev. 1, Idaho National Engineering Laboratories (1997).
17. J. BIRCHLEY, T. Haste and B. Jaeckel, "Pre-Test Analytical Support For Experiments QUENCH-10, -11 and -12," *Proceedings of the International Conference on Nuclear Energy for New Europe (NENE2006)*, Portorož, Slovenia (September 2006).
18. N. B. SOKOLOV, L. N. Andreeva-Andrievska, V. Yu. Vlasov et al., "Genetics of the Interaction of VVER Reactor Core Materials – Recommendations for Use on the Basis of the International Standard Problem on the CORA-W2 Experiment", A A Bochvar All-Russian Scientific Research Institute for Inorganic Materials (VNIINM) Report N8068, Moscow, Russia (1993).
19. J. STUCKERT, Private communication to J. Birchley